University of Alberta
Department of Civil &
Environmental Engineering

Structural Engineering Report No. 66

Some Elementary Mechanics of Explosive and Brittle Failure Modes in Prestressed Containments

by

D.W. Murray

June, 1978

University of Alberta

Department of Civil Engineering

SOME ELEMENTARY MECHANICS OF EXPLOSIVE AND BRITTLE FAILURE MODES IN PRESTRESSED CONTAINMENTS

by

D.W. Murray

A Technical Report to the

Atomic Energy Control Board

Ottawa, Canada K1P 5S9

June, 1978

ABSTRACT

Fundamental concepts related to pneumatic pressurization and 'explosive' behavior of containment structures is reviewed. It is shown that explosive behavior occurs whenever a pressure equal to the ultimate capacity of the structure is attained. The energy associated with hydraulic pressurization is bounded and shown to be orders of magnitude less than that associated with pneumatic pressurization. It is also shown that the structural behavior prior to attaining the ultimate load capacity is independent of the pressurized medium.

The phenomenon of brittle fracture, as it relates to prestressed concrete containments, is explored. A theoretical technique of proportioning cross-sections is developed to eliminate the possibility of catastrophic brittle tensile fractures. The possibility of brittle fractures being triggered by failure of some type of 'detail' is also examined. An attempt is made to identify the types of failures for which the state-of-the-art may be somewhat inadequate to assess behavior under overpressure conditions.

Table of Contents

List of Tables

List of Figures

1. INTRODUCTION

This report has its origins in some simple questions which have been posed with respect to failure modes of prestressed concrete containments when subjected to hypothetical overpressures. The questions have arisen in association with a research project currently underway in the Department of Civil Engineering at the University of Alberta and, in particular, with respect to the difference in behavior to be expected between hydraulic and pneumatic testing of containment structures and the possibility of 'explosive failures'.

There is no question that the 'post-ultimate' behavior of a containment structure will be significantly different as a result of the type of loading to which it is subjected. Simply stated the post-ultimate behavior of a containment structure will be explosive if it is subjected to high gaseous pressure and either (a) a brittle failure occurs, or (b) it reaches its maximum load carrying capacity.

The only way to prevent explosive failure is to ensure that pressure relief occurs prior to attaining the ultimate strength of the structure. The consequences of explosive failure may be variable.

One can postulate a hierarchy of failures. If the failure occurs in a seal, or through an installed pressure relief mechanism, the pressure relief may occur prior to building up destructive pressures and explosive failure may not occur. If a brittle shear type of failure occurs around a penetration, it may result in a projectile being ejected from the wall producing a port large enough to provide pressure relief. Although this may be regarded as an explosive failure, its consequences may be minimal. If the structure maintains sufficient leak-tightness to attain its ultimate capacity, then the failure will be explosive and,

undoubtedly, very destructive. If however, the deformations of the structure are such that they provide sufficient cracking for pressure relief due to leakage prior to attaining the ultimate strength of the structure the failures may be benign.

A philosophy of providing for acceptable behavior under hypothetical overpressures has not yet been evolved, or if it has, has not been communicated to the author. The present philosophy apparently is to design for the maximum credible accident in such a way that no cracking will occur under these conditions. If this argument is accepted it is then unnecessary to consider behavior beyond this point. However, it appears that it would take relatively little effort to provide assurance that catastrophic failure of the structure would not occur in the event of 'incredible' pressures. This could be accomplished by installing pressure relief devices to go into effect at some pressure below the ultimate strength capacity of the structure. Alternatively a non-critical portion of the structure could be consciously designed to fail at a lower pressure than the primary elements of the structure. Present (unverified) indications are that the Gentilly-2 structures would fail in the dome and thus direct any explosive force upwards. However, if this strategy is to be 'successful' the ultimate strength of the cylinder wall should be consciously designed with a higher ultimate strength than the dome. Furthermore, it is necessary to assume that premature failure would not occur due to some detail in the structure.

It is not the purpose, herein, to explore design concepts for 'incredible' accidents. The object of this report is to explore some elementary mechanics related to non-ductile failures. Since it is only the intention to look at the basic mechanics, it is unnecessary to

become involved in many complicating factors which would be necessary if one were to make numerically accurate predictions. The computational aspects of this report have, therefore, been grossly oversimplified in order to focus on conceptual aspects of behavior. It is, however, possible to compute some simple upper bounds which may aid in placing the behavioral aspects in some kind of perspective.

Since the report concentrates on fundamentals, with a view to establishing a common basis on which to carry out more advanced discussions, no attempt is made at providing extensive documentation. No apologies are made for introducing some concepts which may not be directly applicable to prestressed concrete containments, although, in general, an attempt is made to relate the concepts ot the basic problem at hand.

2. DUCTILE AND BRITTLE BEHAVIOR

Ductility is the ability of a material or structure to undergo relatively large inelastic deformations prior to fracture. A ductile material is said to be 'tough' in the sense that the inelastic deformation allows it to absorb large amounts of energy prior to fracture. The difference between ductile and brittle material response is illustrated in Fig. 1 where the brittle material is stronger than the ductile material but is less tough because its energy absorption capacity (represented by the shaded area under the curve) is considerably less than that of the ductile material. Concrete is generally considered to be brittle in tension. Reinforcing steel is considered to be ductile. Prestressing steel, although considerably stronger than reinforcing steel, is less ductile, and hence not as tough.

The above concepts may be transferred directly to the behavior of a structure. It is generally accepted that for a civil engineering structure to perform in a satisfactory manner, it must behave in a ductile fashion. This is usually accomplished by providing higher strengths associated with brittle types of behavior than those associated with ductile types of behavior. Thus, in reinforced concrete design the building codes are written in such a way to provide higher factors of safety for shear failures (brittle behavior) than for flexural failures (ductile behavior). There is also a minimum specified ratio of the area of the tensile reinforcing steel (the ductile component of reinforced concrete) to the concrete area (the brittle component in tension). This aspect of behavior will be the subject of analysis in Sect. 6 of this report. To prevent 'brittle' compressive failures in the concrete, a maximum limit on the percentage of tensile reinforcement is also specified. These

factors are all adequately handled in a properly written code.

There are, however, some conditions in which a ductile material may perform in a brittle manner. The stress-strain plots of Fig. 1 are representative of those obtained under uniaxial stress conditions. The large inelastic uniaxial strain associated with ductility is generally the result of shearing deformations on planes inclined at approximately 45 degrees to the direction of uniaxial stress. If the material is geometrically restrained in such a way that these deformations cannot occur, a biaxial or triaxial state of tensile stress may evolve in which the tensile stresses approach the cleavage strength of the material without accompanying gross deformations. In such a case cleavage fracture may occur in a brittle manner in an ostensibly ductile material. Such cases of high multiaxial tensile stresses often occur around the tips of cracks. The conditions required for the initiation, growth and propagation of cracks gives rise to the specialty area known as fracture mechanics.

While there is a vast body of literature associated with the study of fracture mechanics, most theories can be related to some form of modification of the Griffith's criterion [4,12]. Griffith's basic idea was that a crack will propagate if the elastic strain energy released by the change in stress field resulting from an increase in crack size is equal to or greater than the energy required to produce the incremental change in crack size. Difficulties are encountered in evaluating both of the energy quantities, but in particular the energy required to form the incremental extension of the crack, which generally consists of a combination of a 'surface energy' term and a term representing plastic deformational energy at the crack tips, is difficult to evaluate.

Nevertheless, the concept of such an energy balance is extremely useful in discussing fracture mechanics from a conceptual point of view. It is generally agreed that the energy absoprtion capacity at the tip of a crack in concrete is relatively limited [9] and thus concrete is highly susceptible to the propagation of cracks.

3. CHARACTERISTICS OF LOADINGS AND STRUCTURAL BEHAVIOR

Prior to considering the post-ultimate behavior of a structure it is useful to consider a simple system. The behavior of a structure when subjected to load depends upon the properties of both the structure and the loading. To explore the interaction between these factors it is sufficient to consider the simple beam structure shown in Fig. 2. Fig. 2a illustrates a simple 'reactive loading' system, while Fig. 2b illustrates a 'gravity loading' system. These two loading systems will serve to illustrate a variety of structural responses as characterized by the load-deflection plot shown in Fig. 3.

Let us first discuss the behavior of a ductile structure subjected to a reactive load arising from a hydraulic loading system. The response curve is illustrated by the line O-A-B-C-D of Fig. 3. The load (P_s) applied to the structure may be obtained by taking the product of the hydraulic pressure (p) times the piston area of the hydraulic jack (A_p). Assume first that the hydraulic fluid is incompressible. Let the stiffness of the loading frame be denoted by k_F, as indicated in Fig. 2. For equilibrium of the jack, the force the jack exerts on the loading frame must be equal and opposite to the force the jack exerts on the structure. The force the jack exerts on the loading frame may be considered to be the reaction to the force which the jack exerts on the structure. Thus

$$k_F \Delta_F = p A_p = P_s \tag{3.1}$$

Since it is impossible to exert a force on the structure without the associated reaction, the loading is said to be reactive loading. If

the fluid in the jack is incompressible the jack becomes simply an extensible load transmitting device between the structure and the loading frame.

Consider now the case when the load frame is infinitely rigid in addition to the fluid being incompressible. The reaction is therefore capable of resisting any force with $\Delta_F = 0$. The structural deformation Δ_s then becomes equal to the jack extension and the load transmitted to the reaction is governed by the force with which the structure reacts to the imposed displacement. For a ductile structure the load deformation curve then becomes a characteristic of the structure only. Once the structure deforms beyond its ultimate load position (Δ_u of Fig. 3) there is no difficulty in measuring the load which it can continue to support since the structure simply deforms until it comes into equilibrium with a given pressure on the jack. If the fluid is incompressible, any movement of the structure results in an immediate decrease in the fluid pressure and no further movement of the structure occurs until more fluid is supplied. Therefore, this system is capable of measuring the complete load deformation history of the structure until some element in the structure undergoes a brittle fracture and the structure collapses (point D of the curve). The test may, in fact, be considered to be deformation controlled.

Consider now the behavior of the structure under gravity loading (Fig. 2b). As gravity load is gradually applied, the structure deforms to its equilibrium position and follows the same load deflection path (O-A-B) as for the reactive loading until the structure reaches its maximum load carrying capacity P_u. Assuming there is no mechanism for removing the gravity load, the structure will now collapse. For, given

any deflection exceeding the ultimate deflection, Δ_u, the structure is incapable of providing a reactive force sufficient to counteract the applied gravitational force. In any infinitesimal displacement the work done by the gravitational force exceeds the energy absorbed by the deforming structure. This excess energy is converted into kinetic energy producing an acceleration of the combined load-structure system. The excess energy available for conversion to kinetic energy is indicated by the shaded area in Fig. 3. The sequence of events from the attainment of the ultimate load at B usually occurs rapidly and, although the point of fracture (point D) is reached during the acceleration of the structure, failure may appear to be initiated at point B.

The cases of ideal reactive loading and gravity loading, discussed above, represent limiting cases in the load-structure interaction realtionship. Let us now consider a more realistic simulation of a reactive loading test. Assume the fluid in the jack is incompressible. Assume also that the structure is completely ductile. That is, that the structure does not fracture in a brittle manner at D but is capable of continuing deformation under decreasing load as indicated by the dashed line progressing from D. The support system for the jack normally consists of a loading frame which is subject to only elastic deformation in reacting to the load. Let the stiffness of this system, denoted by k_F, now be a finite quantity. As the jack is extended, a nonzero frame deflection, Δ_F, occurs as well as a nonzero Δ_S, as illustrated in Fig. 2. Since the loading system is again reactive, the Δ_F deflection has no effect on the load-deflection response of Fig. 3 in the region O-A-B-C-D. However the loading frame now possesses strain energy. Assume that at point D the slope of the structural response curve becomes equal to the

negative of the stiffness of the loading frame. The force in the loading frame has precisely the value P_{F2} since it equilibrates the load on the structure. However for a small increment in Δ_{F2} from point D, the force in the loading frame follows a straight line of slope $(-k_{F2})$ while the capacity of the structure to resist load decreases somewhat faster because of the curvature of its load deflection relationship. Point D then becomes a point of instability beyond which the structure cannot absorb energy as fast as the loading frame can release it. The result is that the structure begins to accelerate at point D - i.e. it collapses, even though it still remains ductile.

It has just been demonstrated that for any given structure the structural response curve that one is able to observe beyond the ultimate load condition is a function of the stiffness of the loading frame. Thus, if a more flexible frame, of stiffness k_{F1}, is used the structure would collapse at point C, i.e. - at load P_{F1} rather than load P_{F2}. In the limit, if an extremely flexible loading system is used, the behavior of the structure will be identical to that observed for gravity load, namely, the structure will collapse at point B, following the response path O-A-B-E.

The principles of load-structure interaction are well-known and are considered in any well designed set of tests. The extended solid curve of Fig. 3 is a characteristic of the structure only. However, the portion of the curve which it is possible to observe beyond point B is dependent on the loading system. When post-ultimate strength is desired, a 'hard' test set-up is required. Sometimes, however, it is impossible, even in a well constructed testing machine to obtain sufficient hardness and/or deformation control to obtain the type of

results required. Under these conditions the test specimen may be enclosed in a special stiffening frame as, for instance, in the testing by Evans and Marathe [5] to determine tensile stress-strain curves of concrete beyond the peak stress.

4. PNEUMATIC TESTING OF THE U. OF A. TEST STRUCTURE

Consider now the test system of Fig. 2 in which the loading frame is considered to be infinitely stiff, but the fluid in the jack is compressible. The argument of Sect. 3 may be repeated, essentially verbatim, in which the compressibility of the fluid system replaces the compressibility of the loading frame. In fact the compressibility in the fluid system is rather difficult to determine since it contains flexible hoses, storage chambers, pumps, etc. When both the flexibility of the loading frame and the fluid system are considered, it is the sum of the flexibilities of the two systems which will determine the point of tangency at which 'failure' (i.e. the commencement of structural acceleration) will occur. Since air is very compressible the effect is essentially that of a zero effective k_F stiffness - i.e. a pneumatic system behaves as a 'gravity loading' system except that the pneumatic load can 'follow' the structure in any direction. This can be demonstrated as follows.

Let us illustrate the characteristics of a pneumatic loading on the U. of A. test structure. For any structure which is loaded with an internal pneumatic pressure (p) the incremental work associated with an incremental set of deformations may be expressed as

$$\Delta W = p\, \Delta V \tag{4.1}$$

in which ΔW = the work done by the loading system and ΔV is the increase in internal volume of the structure. The energies associated with such a structure-loading system can, therefore, be interpreted precisely as in Fig. 3 if the y axis (load axis) is interpreted as pressure (p) and

the x axis (deformation axis) is interpreted as volume change (V).

Let us now make some assumptions with respect to the thermodynamics in order to simplify computations. The characteristics of behavior will not be affected by these simplifications. We assume that air will follow an ideal gas law within the limits of our pressurization [20, pg.2-18], that any expansion will be isentropic, and that moisture effects can be neglected. Under such conditions the work done in expanding from pressure p_2 to p_1 is [10, pg.102]:

$$W = \frac{p_1 v_1}{k - 1} \left\{ 1 - \left(\frac{p_2}{p_1}\right)^{\frac{k-1}{k}} \right\} \tag{4.2}$$

and any final pressure may be expressed as

$$p_2 = p_1 \left(\frac{v_1}{v_2}\right)^k \tag{4.3}$$

where k = 1.4 for air. Pressures in these equations are absolute.

Eqs. 4.1 to 4.3 are sufficient for a simple analysis of the problem. The ultimate strain of the prestressing cables is around 4%. Assuming a bounding condition in which the structure undergoes a homogeneous strain of $\varepsilon_u = 0.04$ (an obvious overestimation since the entire structure could not be strained to this extent) the volume change is $3\varepsilon_u = 0.12$. The pressure reduction (assuming no further source of gas during expansion) would be, by Eq. 4.3,

$$p_2 = p_1 \left(\frac{1.0}{1.12}\right)^{1.4} = 0.85\ p_1$$

The maximum pressure reduction during the complete load-deformation

history of the structure would then be 15%. Because air will be continuously supplied to maintain pressure, allowing the maximum possible reduction in pressure, by assuming all strain occurs only after all gas is placed in the initial volume, is certainly nonconservative from a point of view of structural safety and a more realistic assessment (ignoring leakage) would be to assume no pressure reduction during expansion from the ultimate load state. In other words, the characteristics of pneumatic loading are closely represented by the 'gravity' type of load simulation as represented by the O-A-B-E on Fig. 3.

Let us now look at post-ultimate behavior. The energy contained in the loading system at ultimate load may be determined by the work the air would perform in expanding back to atmospheric pressure. This can be obtained from Eq. 4.2. Table 1 indicates the energy available for release from each cubic foot of air for various pressurizations up to 100 psi. Multiplying these figures by the internal volume of the test structure, the energy available to deform and accelerate the structure, in deformations deyond the ultimate capacity of the structure, may be obtained. These figures are also shown in Table 1. To gain some perspective on these figures it is assumed that this energy is converted to kinetic energy in the dome during failure and the theoretical height that the dome roof would reach prior to its descent back to earth ($h_{equ.}$) is shown in the Table. Although this is obviously a simpleminded computation since it ignores post-ultimate energy dissipation within the structure (i.e., the area B-C-D-F-Δ_u-B on Fig. 3), and assumes total transfer of energy, it is indicative of what would happen to the structure once it reaches its maximum capacity.

The conclusion is inescapable. The structure would explode

violently unless the pressure were relieved prior to the attainment of its ultimate loading. It is clearly unacceptable for the current testing to be carried out with pneumatic pressure. Furthermore, it is the author's opinion that no useful information on structural behavior could be obtained from pneumatic tests that is not available from hydraulic tests. If the primary concern is to determine structural response, this response will be similar under both types of loading up to the ultimate load capacity. Pneumatic testing could only be justified in the context of structure-leakage interaction studies.

5. HYDRAULIC TESTING OF THE U. OF A. TEST STRUCTURE

An analysis similar to that carried out in Sect. 4 can also be carried out for hydraulic loading. The results from such an approximation are highly dependent upon the assumptions made in the anlaysis and the object is, again, to obtain simple analyses that yield order-of-magnitude approximations rather than numerically accurate results.

The analysis for hydraulic loading will be carried out by bounding the energy from above and from below. For a test structure pressurized with water an upper bound on the energy may be obtained by assuming the water to be saturated with as much air as it can hold in solution. For this purpose it will be assumed that Henry's Law is valid. Henry's Law states that the mole fraction of the solute in the solvent is proportional to the absolute pressure. Thus we may write [18]

$$x_a = p/H \tag{5.1}$$

where x_a is the mole fraction, p is the absolute pressure (in atmospheres) and H is Henry's constant, tabulated as 6.64×10^4 [Table 3-123, pg. 3-96, Ref. 18]. For 100 psig (114.7 psia, or 7.803 atmo.) the mole fraction is

$$x_a = 7.803/(6.64 \times 10^4) = 117.5 \times 10^{-6} \text{ moles/mole.}$$

Assuming the molecular weight of air m_a is 28.97 [pg.96, Ref. 10] and that of water m_w is 18.02 the weight of air in water is obtained as (Eq. 14-3, Ref. 18)

$$w(\text{lb.air/lb.water}) = \frac{x_a}{1 - x_a}\left(\frac{m_a}{m_w}\right) \qquad (5.2)$$

$$= 117.5 \times 10^{-6} \times 28.97/18.02$$

$$= 188.9 \times 10^{-6}$$

Using a unit weight of air of 0.0753 lb./ft.^{3} at 20°C and atmospheric pressure, and assuming water at 62.4 lb./ft.^{3} yields

Vol. of air referenced to 20°C and 1 atmos./ft.^{3} water

$$= \frac{188.9 \times 10^{-6}}{0.0753} \times 62.4 = 0.156 \frac{\text{ft.}^3 \text{ air}}{\text{ft.}^3 \text{ water}}$$

Similar values are tabulated in column 2 of Table 2 for various containment pressures.

The maximum volume of air that could come out of solution during depressurization is represented by the difference between the numbers tabulated in column 2 and that number tabulated for 0 psig pressure in column 2. Forming this difference and multiplying by the volume of the structure (851 ft.^{3}) yields the total quantity of air that would come out of solution during depressurization (column 3 of Table 2). The corresponding volume, after pressurization, computed by the ideal gas law and assuming isothermal conditions, is shown in column 4 of Table 2. (It can be argued that, since the water is a large heat sink, isothermal conditions are more applicable to this condition than isentropic conditions).

An 'exact' formulation for the work done during expansion as the gas comes out of solution could now be carried out. However, it will be argued that since, in the case of a pressure of 100 psig, 115.7 ft.^{3} of air will come out of solution, an order-of-magnitude computation for the work done by this expanding gas can be obtained by separating the gas from the liquid and considering the work done by an isothermal expansion of the gas only, between the pressures of 100 psig and 0 psig. The formula for work done during this expansion is

$$Wk = p_2 \, v_2 \, \ln \left(\frac{p_1}{p_2}\right) \tag{5.3}$$

when the subscripts 1 and 2 indicate initial and final conditions, respectively. Column 5 indicates the energy release of the dissolved gas for the respective expansions computed according to Eq. 5.3. Column 6 converts this energy to a potential energy of the dome. These figures represent upper bounds on the effect of the pressurizing medium, not only because they assume the water is completely saturated and for the reasons stated in the previous section, but also because they neglect the time which is required for the gas to come out of solution.

A comparison of Table 2 with Table 1 indicates that testing with air saturated water reduces the equivalent h to about 3% of that for pneumatic testing. However, the energy in the test medium is still at a destructive level and could lead to explosive failures. In comparison, the energy stored when pure water is used as the pressurizing medium is computed (by interpolation of volume changes) in Table 3. Again the precise figures are unimportant but it is apparent that failure

is benign in comparison with the pneumatic and the saturated water systems.

The conclusion that can be reached from the analysis above and that of Sect. 4 is that, unless special bunker type facilities are built (this has been done, for instance, in Italy) containment structures should be tested hydraulically. Furthermore, in any hydraulic test it is essential that steps be taken to avoid entrapped and dissolved air in the system. It should be noted that the hydraulic tests of containments carried out in Italy failed explosively, although it must also be noted that they failed at much higher pressures (2000 to 3000 psig) and had unbonded tendons. (Note: Documentation in the literature of these tests is very incomplete, see, e.g. Ref. 7. However, a motion picture of these tests shown at the SMIRT4 Conference in San Francisco, August, 1977, indicated that explosive failures had occurred).

6. CHARACTERISTICS OF BRITTLE TENSILE FAILURES

The preceding analyses assume that the structure will exhibit ductile response throughout the loading. An explosive failure, under gaseous internal pressure, would then occur at the pressure at which the load carrying capacity of the structure begins to decrease. However, if a brittle fracture were to occur at a lower load level, such as point A of Fig. 3, an explosive failure could result prior to attaining the maximum carrying capacity of the structure. That is, a brittle fracture would allow a sudden release of the energy of the pressurized medium contained within the structure at the time of propagation of the fracture.

The classical brittle fracture phenomenon is such that once a crack reaches a certain critical size it propagates through the entire structure at approximately the speed of sound in the fracturing medium. One may postulate that this occurs when concrete reaches its maximum tensile strength. It should be noted that the writer does not consider this classical concept to be applicable to concrete structures, and there has been no evidence to support such behavior in the current test series. However, we will proceed with a description of a simple analysis of brittle fracture behavior in order to demonstrate its consequences and will follow in Sect. 7 with a technique for ensuring that it does not result in catastrophic collapse. While concrete may be assumed to behave in a brittle manner, the steel components (both reinforcement and prestressing tendons) will not. The steel, therefore, serves to constrain the deformation of the structure unless the net energy released by the formation of the crack is sufficient to exhaust the energy absorption capacity of the steel.

Considering the above statement as a modified Griffith's concept, bounds on the effect of brittle concrete failure may be obtained as follows. We illustrate the analysis on a simple membrane element as indicated in Fig. 4. (A similar type of analysis may be carried out for flexure or combined flexure and membrane forces). As a limiting case we assume that upon formation of the crack the concrete stress normal to the crack reduces to zero throughout the element (the 'tension cut-off' assumption), and that the surface energy and plastic deformational energy associated with the crack formation are negligible. Furthermore, it will be assumed that the stress-strain properties of the steel are bilinear as shown in Fig. 5. More realistic properties for the steel can easily be used but simply complicate the formulation while not contributing to the conceptual arguments.

The analysis of the consequences of a brittle fracture of the concrete may now be undertaken using the type of energy arguments advanced for ductile failures in Sects. 3 and 4. Let us first consider the behavior of the cracked segment, for which only the steel is effective in tension. Let us also assume that the prestressing tendons are prestressed. Under these conditions the load-deflection plot of the segment of Fig. 4 is shown as the line E-B-C-D of Fig. 6a. The critical points on this curve may be obtained as follows. The deformation of the segment (Δ of Fig. 4) is measured with respect to the reference configuration which exists after prestressing but prior to application of the external load P, which is assumed to arise from internal pressurization. In the initial configuration the stress in the prestressing steel is denoted by f_{pi} (approximately 0.6 f_{pu}) and that in the reinforcement is denoted by f_{si}, as indicated on Fig. 5. Strains and stresses produced by the

elongation Δ must then be referenced to the initial stress points a and b indicated on Fig. 5, and the force in all steel, P_s, for an arbitrary (pre-yield) elongation Δ may be expressed as

$$P_s = A_p(f_{pi} + E_p \Delta/L) + A_s(f_{si} + E_s \Delta/L) \qquad (6.1)$$

where A and E represent the respective areas and elastic moduli, as distinguished by the subscripts p for prestressing and s for reinforcing steel. Eq. 6.1 is valid only for $\Delta > 0$.

When $\Delta = 0$, the initial force in the steel, P_{si}, is obtained from Eq. 6.1 as

$$P_{si} = A_p f_{pi} + A_s f_{si} \qquad (6.2)$$

The reinforcement yields when the right hand bracket in Eq. 6.1 reaches f_{sy}. This condition gives the solution of Δ at first yield, in the form

$$\Delta_y = \frac{L}{E_s}(f_{sy} - f_{si}) \qquad (6.3)$$

at which deflection, Eq. 6.1 gives the yield load as

$$P_y = A_p \left\{ f_{pi} + \frac{E_p}{E_s}(f_{sy} - f_{si}) \right\} + A_s f_{sy} \qquad (6.4)$$

The prestressing steel reaches its ultimate strength when the left bracket of Eq. 6.1 reaches f_{pu}. This condition permits the solution for Δ_u in the form

$$\Delta_u = \frac{L}{E_p} (f_{pu} - f_{pi}) \tag{6.5}$$

at which time the ultimate load on the section, P_u, may be evaluated from Eq. 6.1 as

$$P_u = A_p f_{pu} + A_s f_{sy} \tag{6.6}$$

The above critical points P_{si}, P_y and P_u are plotted as points E, B and C, respectively, on Fig. 6a.

The stiffnesses of the 'steel-only' segment may be obtained as

$$k_{s1} = (P_y - P_{si})/\Delta_y = (A_p E_p + A_s E_s)/L \tag{6.7}$$

and

$$k_{s2} = (P_u - P_y)/(\Delta_u - \Delta_y) = E_p A_p/L \tag{6.8}$$

as indicated on Fig. 6a.

The total external force on the uncracked section, P, may now be expressed as the sum of that in the concrete, P_c, and that in the steel, P_s, to yield

$$P = P_c + P_s \tag{6.9}$$

and the stiffness of the uncracked section is

$$k_T = P/\Delta = (A_c E_c^* + A_s E_s + A_p E_p)/L \tag{6.10}$$

where E_c^* is the 'effective' modulus of the concrete recognizing the biaxial stress condition implied by Fig. 4. Note that when $\Delta = 0$ the total force is zero and Eq. 6.9 yields

$$P_{ci} = -P_{si} \tag{6.11}$$

Let us now consider the idealized behavior of the segment as external load is applied and assuming the tensile strength of the concrete is zero. The response may be traced on Fig. 6a as follows. As the segment is deformed the external load moves up the line O-A, with the stiffness k_T of Eq. 6.10. At point A, the external load is balanced by the force in the steel only; i.e. - the stress in the concrete becomes zero. Since concrete cannot resist tension, the load deformation response subsequently follows along line A-B, with the stiffness k_{s1} of Eq. 6.7, until the reinforcement yields at point B. For further deformation only the prestressing steel increases in stress and the response follows the line B-C, with the stiffness k_{s2} of Eq. 6.8. The ultimate strength is attained at point C. Assuming a rigid reactive loading system, this ultimate load can be maintained until the prestressing steel reaches its maximum strain, at point D, at which point a cleavage fracture of the tendon occurs.

Now that the reactive load-deflection response has been determined it is relatively straight forward to investigate the consequences of brittle concrete fracture under pneumatic loading. Areas under the load-deflection plot of Fig. 6a represent energies, just as in the discussions of Sect. 3. In the present analysis it is only energy differences which are significant and these are represented by the

difference in areas between the loading and resisting curves. If the load is assumed to arise from pneumatic loading it has the characteristics of a gravity load as discussed in Sect. 4.

Assume now that the concrete has a finite tensile strength f_t. Loading of the structure follows the line O-A and continues at this stiffness until the cracking load is reached at point F. The cracking load may be evaluated from the equation for total load

$$P = A_c(f_{ci} + E_c^* \frac{\Delta}{L}) + A_p(f_{pi} + E_p \frac{\Delta}{L}) + A_s(f_{si} + E_s \frac{\Delta}{L}) \quad (6.12)$$

when the left hand bracket reaches f_t. Solving for the cracking elongation, Δ_{cr}, by equating the left hand bracket in Eq. 6.12 to f_t, yields

$$\Delta_{cr} = \frac{L}{E_c^*}(f_t - f_{ci}) \quad (6.13)$$

at which elongation, Eq. 6.12 yields

$$P_{cr} = A_c f_t + A_p \left\{ f_{pi} + \frac{E_p}{E_c^*}(f_t - f_{ci}) \right\} + A_s \left\{ f_{si} + \frac{E_s}{E_c^*}(f_t - f_{ci}) \right\} \quad (6.14)$$

Since the load is pneumatic, this (external) load remains constant upon brittle failure of the concrete. At cracking the segment suddenly reverts to a 'steel-only' section according to our simplifying assumption. If the load P_{cr} were slowly applied to a section, without concrete tensile strength, it would be in equilibrium at point G along the path A-B as

previously discussed. However, the excess energy now transmitted to the segment by the external load, and represented by the horizontally shaded area A-F-G, is converted to kinetic energy and the segment will continue to deform until this excess energy is stored as strain energy or dissipated in plastic deformation. The segment will, therefore, develop an 'impact loading' in excess of that anticipated by static loading, deforming to point J, at which time the area G-B-J-K becomes equal to A-F-G. If this 'impact' effect carries the segment past the yield load, P_y, a permanent set in the reinforcement occurs and the ultimate equilibrium position becomes G' once the strain energy G'-J-K is dissipated through vibratory motion. The energy G-B-J-G' is absorbed by the plastic deformation. Upon unloading, the segment would follow the load-path G'-A'-O.

For the segment response illustrated in Fig. 6a, brittle fracture of the concrete would be constrained by the ductile steel components. However, the relative locations of the points on the behavior curves depend on the composition of the cross-section. If the concrete tensile strength were high, and the section were lightly reinforced, an energy relationship of the type shown in Fig. 6b could occur. In this case the ductile elements do not absorb sufficient energy to counteract the energy release upon cracking of the concrete. The result would be an explosive failure triggered by brittle fracture of the concrete prior to reaching the static load-carrying capacity of the structure, since the absorbed energy would never become large enough to balance the supplied energy. This is one mechanism by which a brittle failure could occur at a point such as A on Fig. 3. An unfavorable balance of components of this type has previously been pointed out in a noncritical area of the G-2 design [15].

An analysis of the above type can, of course, be carried out for more complex steel properties provided that the load-deformation curve of the 'steel-only' section is adjusted. It may also be carried out for different types of stress-resultants or combinations of stress resultants. The anlaysis is independent of length and therefore may be applied to the entire structure or any segment of the structure. The Achilles heel of the argument rests on two assumptions. First, it assumes that there is no reduction in load as the structure deforms. It was demonstrated in Sect. 4 that this assumption is a good one for membrane forces arising from pneumatic pressures. However, for moments the assumption is questionable because the increments in curvature are geometrically constrained. Second, the argument assumes that a crack forms suddenly, and in a brittle manner, in such a way that the concrete stress over some finite length reduces to zero. If L of Fig. 4 represents this length, the implication is that, if the test were deflection controlled, the load, upon cracking, would drop precipitously from point F to point F' of Fig. 6a. Although deformation controlled tests have not been run in the laboratory, and indeed would be difficult to carry out because of the softness of the loading system (see Sect. 3), the writer considers this behavior to be extremely unlikely and, indeed, it has not been observed in other types of cracking in reinforced concrete. Hence, the behavior predicted by this brittle fracture type of analysis can be considered to represent only a theoretical bound on the response that might occur.

Table 4 contains a summary of the equations derived in this section.

7. ARRESTING BRITTLE TENSILE FAILURES

It is a relatively simple matter to proportion a cross-section so that brittle fractures of the type postulated in Sect. 6 are constrained in their behavior. For instance, suppose that it is desirable to prevent yielding of the non-prestressed steel due to the 'impact' effect of cracking. This can be accomplished by keeping point J of Figs. 6a and 7a below point B. This is true if the Area G-K-J is greater than the Area A-G-F, when point J coincides with point B.

To simplify the algebra, and still remain conservative, let us require that Area J-K-G be greater than or equal to Area A-M-G of Fig. 7a, when point J coincides with point B. The stress difference in the concrete between P_o and P_{cr} is the tensile strength of the concrete, f_t. Then Area A-M-G is proportional to AM which is

$$P_{cr} - P_o = (A_c + n\,A_s + n\,A_p)\,f_t \qquad (7.1)$$

(Note that henceforth it is assumed that $E_s = E_p$ and $n = E_s/E_c^* = E_p/E_c^*$). Similarly since (neglecting creep) $f_c = f_s = 0$ at P_o,

$$P_y - P_o = (A_s + A_p)\,f_{sy} \qquad (7.2)$$

Subtracting Eq. 7.1 from Eq. 7.2 yields

$$P_y - P_{cr} = (A_s + A_p)\,f_{sy} - (A_c + n\,A_s + n\,A_p)\,f_t \qquad (7.3)$$

Now for no yielding

$$P_y - P_{cr} \geq P_{cr} - P_o \tag{7.4a}$$

or, upon substituting Eqs. 7.1 and 7.3, into Eq. 7.4a,

$$(A_s + A_p)\, f_{sy} \geq 2(A_c + n\, A_s + n\, A_p)\, f_t \tag{7.4b}$$

or $$(A_s + A_p)(f_{sy} - 2\, n\, f_t) \geq 2\, A_c\, f_t \tag{7.4c}$$

Defining the total percentage of reinforcing, ρ_g, as

$$\rho_g = (A_s + A_p)/A_c \tag{7.5}$$

Eq. 7.4c can be written as

$$\rho_g \geq 1/(f_{sy}/2\, f_t - n) \tag{7.6}$$

Eq. 7.6 indicates that if yielding is not to occur in the event of a brittle concrete fracture, the percentage of total steel must be kept greater than a minimum, which depends on the ratio of the moduli of elasticity and the 'strengths' of the materials. This equation is, of course, considerably oversimplified, because of the material property assumptions, but is indicative of the type of restrictions which must be placed on the proportioning of the cross-sectional components in order to be assured that steel yielding does not occur upon brittle fracture of the concrete.

A similar type of analysis may be carried out to ensure that the ultimate strength capacity of the section is not exceeded in the

event of a brittle failure of the concrete. The energy balance is illustrated in Fig. 7b, and expressed by the equation

$$\frac{1}{2} P_{yo} \varepsilon_{uo} + \frac{1}{2} P_{uo} \varepsilon_{uy} - P_{cro} \varepsilon_{uo} \geq 0 \qquad (7.7)$$

where the multiple subscripts indicate differences between the variables evaluated at the simple subscripts. Substituting the values from the equations in Table 4 and grouping variables this equation reduces, after some algebraic manipultion, to

$$\rho_s \left[\left(2 - \frac{f_{sy}/f_{pu}}{1 - \beta \xi}\right) \frac{f_{sy}}{f_t} - 2n\right] + \rho_p \left[\frac{f_{pu}}{f_t} (1 - \beta \xi) - 2 n\right] \geq 2 \qquad (7.8)$$

where it is again assumed that $E_s = E_p$; $n = E_s/E_c^*$; $f_{si} = n f_{ci}$; and the following definitions apply

$$\rho_p = A_p/A_c \qquad (7.9a)$$

$$\rho_s = A_s/A_c \qquad (7.9b)$$

$$\beta = f_{pi}/f_{pu} \qquad (7.9c)$$

and $$\xi = [1 + n(\rho_s + \rho_p)]/(1 + n \rho_s) \qquad (7.9d)$$

Knowing either one of the variables ρ_s or ρ_p, Eq. 7.8 may be solved for the minimum required value of the other variable. However, because ξ depends on these variables, Eq. 7.8 is slightly nonlinear and is best

solved iteratively. This has been done for typical values of the variables, and the results are shown in Tables 5 and 6.

To examine the numerical results of this type of theory it is first convenient to look at the requirements of Eq. 7.6 to prevent yielding. These are shown in Table 7. The brittle fracture theory requires a percentage of reinforcement varying from 1.5% to 1.8%, for the range concrete strengths considered, in order to prevent reinforcement yield in the event of sudden concrete fracture. This is a severe requirement and probably economically unfeasible. As an example the wall in the Gentilly-2 containment structure has reinforcement ratios of $\rho_s = 0.00313$ and $\rho_p = 0.00258$ for a combined $\rho_g = 0.00571$ which is approximately one third of that required by this analysis. On the other hand, the dome has ratios of $\rho_s = 0.00708$ and $\rho_p = 0.00809$ for a combined $\rho_g = 0.0152$ which is essentially that required by the analysis for 5000 psi concrete.

To prevent the attainment of the ultimate strength of the prestressing upon brittle fracture of the concrete, reference may be made to Table 5. For wall reinforcing of 0.003 corresponding approximately to 0.00313 in Gentilly-2 the table indicates a required prestressing ratio of 0.00707 as compared to 0.00258 for Gentilly-2 indicating that a brittle fracture of the concrete at this section could trigger collapse. On the other hand for dome reinforcing of 0.007 (compared to 0.00708 in Gentilly-2) the table indicates a required prestressing ratio of 0.00334 (compared to 0.00809 in Gentilly-2) indicating that brittle fracture in the dome would not lead to collapse.

It is apparent that the higher the concrete strength the more severe the criteria for a brittle fracture phenomenon. It is also apparent,

by comparing Table 6 with Table 5, that the less creep in the concrete (i.e. - the higher f_{pi}) the more severe are the brittle fracture requirements. It should be noted that if $f_{pu} = f_{sy}$ and $\beta = 0$, Eq. 7.8 specializes to Eq. 7.6.

8. DETAILS AND BRITTLE FRACTURE

The behavior of a structure can be significantly influenced by the design and construction practices employed in regions of geometric discontinuities, penetrations, termination of reinforcement, etc. Such items will be referred to collectively as 'details'. First signs of structural distress are often associated with details and, generally speaking, the adequacy of detailing practice must be established from testing programs since precise predictions of behavior cannot usually be established analytically.

There has, however, been a long history of investigation associated with many detailing problems for which design rules have been formulated and detailing practice codified. Generally speaking the philosophy of providing adequate details is:

(a) provide a strength at least equal to that of the undisturbed structure so that failure occurs in a region remote from the detail, or

(b) if (a) is not possible, provide strength sufficient to force yielding in regions remote from the detail.

In either case the primary concern is to ensure ductile behavior of the structure as a whole even though the region associated with the detail may be the area where first distress occurs and may participate in the ultimate collapse.

A number of details which may be of concern with respect to weakening the structure are discussed conceptually in the following. Since the subject is large and complex the discussion must remain incomplete. Each design office develops its own practice with respect to these problems and, since practitioners must necessarily possess more

expertise in this respect than the author, the primary intent is to examine characteristics of behavior and isolate possible problems rather than to recommend design procedures.

8.1 'Small' Penetrations

Many small penetrations occur throughout a nuclear containment structure. In steel pressure vessels these are normally handled by the "area replacement rule", [2,13]. This rule basically states that the area removed by the penetration be replaced by an equal area of reinforcement in the vicinity of the penetration. This is adequate for ductile behavior. However, stress concentrations arise around penetrations and these give rise to concern about the possibilities of fatigue failures and brittle fracture failures [3,13]. In secondary containment structures fatigue is not a problem and attention may be focussed on (a) the possibility of brittle fracture, (b) ultimate strength, and (c) the integrity of the containment prior to collapse.

For prestressed concrete secondary containments the initial cracking loads will be influenced by stress concentrations in the vicinity of penetrations. A circular penetration gives rise to a local stress distribution as indicated in Fig. 8a, which has a stress concentration factor (SCF), designated as K_t, of 3 for uniaxial tension. Rectangular penetrations with square corners give rise to infinite stress concentrations, producing cracking at the corners as indicated in Fig. 8b. Numerous publications [8,19,21] give well documented SCF's for a variety of shapes of openings, with and without reinforcement, and under various biaxial stress conditions for isotropic elastic materials. It can be argued that, since creep will reduce the stress concentrations due to

prestress, large tensile stresses could occur in the vicinity of penetrations prior to the development of any significant average tensile stress on the cross-section. On the other hand, Evans and Marathe [6] have demonstrated that, on small specimens, a stress concentration factor of 493 did not reduce the average tensile strength of the concrete. Their argument is that the stress concentrations around microcracks which are naturally present in the concrete, are sufficiently high so that geometrically induced SCF's can essentially be ignored. While not fully supporting this conclusion because of the compounding effect of stress concentration factors [17], there seems little doubt that cracks arising from SCF's are a local phenomenon and should not impair the basic functions of the structure providing that sufficient reinforcing is provided to adequately distribute the cracking. This conclusion appears to be consistent with that reached by the ACI-ASME Technical Committee on Concrete Pressure Components for Nuclear Service which states that "... (stress) limits specified ... may be exceeded for local peak tensile stresses provided ... (a) ... attention is given to any redistribution of stresses ... (c) Reinforcement is provided to control and distribute cracking ...." [1].

Since the reinforcing and prestressing steel serve as ductile components to arrest failure upon cracking of the concrete, as discussed in Sect. 7, the phenomenon of brittle fracture in the classical sense is not a feasible failure mode in concrete containments provided the ultimate strength capacity of the steel is adequate. This aspect of behavior is considered in the following section.

When a section is subjected to moment, in addition to membrane tension, it may be considered to be made up of a series of layers, each

in a plane stress condition. All considerations applicable to membrane stresses may then be applied directly to the combined stress resultant case. The only additional factor to consider is the adequacy of the ultimate strength compression block if such a failure is considered feasible.

8.2 Rows of Penetrations

Rows of penetrations may produce two effects. First, they may reduce the stiffness in the area of the penetrations. Second, they give rise to a series of stress concentrations. The effect of reducing the stiffness is illustrated in Fig. 9, where the net section on Sect. A-A is assumed to be significantly reduced by a series of penetrations in the concrete. The result is that the centrally located pressure load is eccentric from the centroid of the resisting area, and consequently a moment equal to the total force times the distance between the axis of symmetry and the centroid (e of Fig. 9b) is created on the net section. The average stress on the section is then increased in the ratio A_G/A_N (where subscripts G and N denote 'gross' and 'net' areas, respectively) and the stress on the weaker side is further increased by the factor $P \cdot e \cdot y/I_N$, where y is the distance from the centroidal axis to the point under consideration. Any stress concentration effect is applied to this increased stress level.

For a single small penetration, which subtends an angle of $\Delta\theta$ at the axis of symmetry, the ratio of the increased stress, σ^*, to that in the undisturbed structure, σ, may be approximated (for $\Delta\theta \leq 0.2$) as

$$\frac{\sigma^*}{\sigma} = \frac{1}{(1 - \Delta\theta/2\pi)} \left\{1 + \frac{\Delta\theta}{(1 - \Delta\theta/2\pi)(\pi - \Delta\theta)}\right\} \qquad (8.1)$$

For a structure of the dimensions of Gentilly-2 a four foot penetration results in a stress increase of approximately 3%. For a row of penetrations, such as illustrated in Fig. 9b, the effect would be more pronounced.

This eccentricity effect could be eliminated by the "area replacement rule". This can be accomplished either by providing a steel sleeve of thickness approximately 1/10 the radius of the hole (the ratio comes from the modular ratio [6]) or by providing an equivalent amount of reinforcing steel. However, neither of these solutions appears to be economical, or even desirable, for any but the smallest of penetrations. In the first case there is a serious question about the effectiveness of the sleeve because of problems with bond. The second solution would, therefore, appear to be preferable but would lead to undesirable concentrations of reinforcing. A suitable detail would undoubtedly arise if the reinforcing steel was increased to account for the effects of eccentricity, a sleeve of nominal diameter was provided, and distribution steel for stress concentration effects, as discussed in Sect. 8.1, was also provided.

It should be noted that the ultimate tensile strength of the section is a function of the area of steel only. The ultimate strength is, therefore, not reduced as a result of the penetrations if the steel passing through the net section is greater than or equivalent to that in the undisturbed structure. Since strain concentrations will occur in the vicinity of the penetration, first fracture of the steel, as well as first cracking of the concrete, may occur on a section adjacent to a penetration.

This should not be a significant concern providing the ultimate strength on the net section is sufficient to force general yielding in areas remote from the concentration.

If yielding of the structure is not forced at sections remote from the penetrations, the structure as a whole could respond in a brittle fashion. That is, concentrations of strain at the net section could exhaust the ductility of the steel locally prior to general yielding.

To prevent such undesirable behavior at net sections it is necessary to satisfy two inequalities in addition to those discussed in Sect. 7. Using the subscripts N and G to denote net and gross sections, respectively, (illustrated by sections A-A and B-B of Fig. 10), the ultimate strength requirement on the net section is (from Eq. 6.6)

$$[f_{sy} A_s + f_{pu} A_p]_N \geq [f_{sy} A_s + f_{pu} A_p]_G \tag{8.2}$$

The requirement to force cracking on sections remote from the detail is (from Eqs. 6.6 and 6.14)

$$[f_{sy} A_s + f_{pu} A_p]_N \geq [A_c f_t + A_p \left\{ f_{pi} + \frac{E_p}{E_c^*} (f_t - f_{ci}) \right\} + A_s \left\{ f_{si} + \frac{E_s}{E_c^*} (f_t - f_{ci}) \right\}]_G \tag{8.3}$$

If the inequalities 8.2 and 8.3 are both satisfied general yielding is also assured.

8.3 Shear

A rational analysis of shear behavior in reinforced and prestressed concrete has continued to elude engineers in spite of the many attempts to resolve the problem over several decades. Although the mechanisms of failure are reasonably well understood conceptually, the evaluation of strength remains largely based upon parameters statistically derived from a large number of tests. Tests have been carried out on a variety of standard types of structural elements and design rules adjusted to suit the particular application.

Generally the shear-cracking strength of a structural element is dependent upon the tensile strength of the concrete. The post-cracking behavior is dependent upon: (a) the compression block in the concrete, (b) shearing reinforcement, (c) aggregate interlock across the cracks, and (d) dowel action across the cracks. In normal beam design, items (c) and (d) are neglected. In some applications aggregate interlock or 'shear friction' is counted on.

Since a Gentilly-2 type containment structure carries its loads primarily by membrane action the levels of shearing stress are generally low. They may arise from two effects, namely, (i) enforcement of geometric compatibility in zones of geometric discontinuity ('compatibility shears'), and (ii) the application of concentrated or line loads ('load shears').

Once a structure enters a state of membrane tension sufficient to cause through-cracking of the concrete the major method of resisting shearing forces is to provide shearing reinforcement. Shear friction would only be applicable if the reinforcement did not strain sufficiently to allow large crack widths. Therefore, if it is desired to prevent shear

failures prior to the development of the ultimate flexure-membrane capacity of the structure, shear reinforcement is probably required around those penetrations subject to concentrated loads and in regions of compatibility shear, at least in those areas where the flexure-membrane analysis predicts a through-cracking condition.

The above requirement is unusual for reinforced concrete structures and arises because the overload stress conditions in a containment are not those found in most reinforced concrete applications. Experience and testing programs may establish that adequate shear capacity exists around penetrations due to deformation of the membrane tension field and aggregate interlock or dowel action. In the meantime standard techniques of providing for shear are the only tools available for assessing behavior.

It should be noted that some success has been achieved at the University of Illinois in predicting shear failures using finite element tension cut-off analyses. Shear failures, in the absence of shear reinforcing are brittle. However, the consequences of a shear failure in a G-2 type containment structure remain to be determined.

8.4 Reinforcement Bond and Anchorage

The behavior of the structure predicted by any analytical technique assumes that it is possible to develop the yield or ultimate strength of the steel reinforcement. In order for the reinforcement to develop this stress it is necessary for a transfer of stress to occur between the steel and concrete, as illustrated in Fig. 11a. This stress is referred to as bond stress and the length of embedded bar required to develop the desired stress in the bar is referred to as the anchorage

or development length. Due to the deformations on the bar a wedging action is set up which grips the bar but, in turn, tends to split the concrete. This splitting marks the start of bond failure. Transverse reinforcement will tend to restrict the opening of the splitting cracks once they have formed, delaying the final failure a little [16].

The capability of developing bond stress is influenced by the normal stress on planes parallel to the axis of the reinforcement. Cracking on these planes, as illustrated in Fig. 11a, should reduce or eliminate the capacity of the concrete to transfer bond stresses depending on the amount of transverse reinforcement. A similar phenomenon occurs in lap splices as illustrated in Fig. 11b.

Since overload pressures produce states of biaxial tensile stresses in containment structures, bond failure could occur prior to the development of the full yield strength of the reinforcement resulting in brittle behavior of the overall structure at loads below those predicted by analysis.

Concern for this type of failure has led to the following clause in the ASME Code for Concrete Reactor Vessels and Containments [1].

> "CC-3532 ....
> (c) Where a nonprestressed reinforcement bar splice must be located in a region where tension is predicted in a direction perpendicular to the bar to be spliced, only a full positive mechanical splice or a full welded splice shall be used unless calculations or tests of the selected splice detail are made to demonstrate that there is adequate transfer of force. ..."

The current test series on wall segments at the University of Alberta contains two specimens with lapped splices. Some indication of whether such splices lead to premature failure should be obtained from

these tests. In the meantime the area of reinforcement splicing should be identified as one which may be a cause for concern in the overload behavior of containment structures.

8.5 Large Openings

The problems associated with large openings must be dealt with on an individual basis.

9. CLOSURE

This report has attempted a cursory examination of various types of failure modes that may occur in association with concrete containment structures, with a view to examining some of the fundamental mechanics associated with these failures, and with particular reference to brittle and explosive behavior.

The following may be considered a brief summary of some of the major points.

1. Ductile behavior does not ensure that 'explosive' behavior will not occur. 'Explosive' behavior can be expected when the maximum load carrying capacity of the structure under internal pneumatic pressure is reached, unless pressure relief is achieved through other means prior to this point (Sects. 3 and 4).
2. Information on structural response obtained through hydraulic testing is valid for prediction of behavior under pneumatic loading (Sect. 3). Without special facilities pneumatic loading is dangerous and should be avoided (Sects. 4 and 5).
3. Brittle failure of the overall structure, leading to premature explosive behavior, can be avoided by ensuring that the structure is properly detailed. In particular, the possibility of brittle tensile failures occurring can be eliminated by providing sufficient reinforcement (Sect. 7). However, there is (apparently) no experimental evidence that this type of failure occurs in reinforced or prestressed concrete structures.
4. Penetrations introduce (a) local peak stresses and (b) a general increase in the stress level due to displacement of

the center of resistance. However, they do not decrease the ultimate strength of a tensile structure providing sufficient effective area of reinforcement is maintained. The principal concerns associated with (unloaded) penetrations are, therefore, to ensure adequate behavior at service loads and to ensure that sections containing penetrations have sufficient strength to force yielding at sections remote from the penetrations (Sects. 8.1 and 8.2). This is primarily a matter of adequate detailing.

5. Shear failures are brittle and could result in premature failure in the vicinity of loaded penetrations and geometric discontinuities. Normally in regions of geometric discontinuity there is sufficint moment to provide a compression block which inhibits shear failure. However, to the author's knowledge, no adequate design techniques exist at present for tension structures other than providing transverse shear reinforcement (Sect. 8.3).

6. Bond failures could trigger brittle fracture of the structure. Dr. J.G. MacGregor is testing some tensile specimens with lapped splices in association with Phase II of this investigation, and will report his conclusions when these tests are complete. In the meantime, the detailing practice associated with reinforcement splices remains an area of concern.

In any report such as this it is impossible to cover all possibilities associated with structural failure. The obvious failure mode, that of ductile general yielding, has barely been mentioned since

it is the subject of detailed study elsewhere. However, it is hoped that this report will have served a useful purpose in pointing out some fundamentals associated with possible failure modes other than general ductile yielding.

REFERENCES

1. "ASME Boiler and Pressure Vessel Code: Section III - Division 2: Code for Concrete Reactor Vessels and Containments (ACI Standard 359-74)", 1975 Edition, ASME, 345 East Forty-Seventh Street, New York, N.Y., 10017.

2. "ASME Boiler and Pressure Vessel Code: Section I - Rules for Construction of Power Boilers", 1968 Edition, ASME, 345 East Forty-Seventh Street, New York, N.Y., 10017, pp. 32-44.

3. "Criteria of the ASME Boiler and Pressure Vessel Code for Design and Analysis by Sections III and VIII, Division 2", in Pressure Vessels and Piping - A Decade of Progress - Vol. 1, ASME, 345 East Forty-Seventh Street, New York, N.Y., 1972, pp. 61-83.

4. Dieter, G.E., "Mechanical Metallurgy", McGraw-Hill Book Co., 1961.

5. Evans, R.H. and Marathe, M.S., "Microcracking and Stress-Strain Curves for concrete in Tension", Materials and Structures, Vol. 1, No. 1, Jan. - Feb. 1968, pp. 61-64.

6. Evans, R.H. and Marathe, M.S., "Stress Concentrations in Prestressed Concrete", Conference on Prestressed Concrete Pressure Vessels, The Institute of Civil Engineers, London, 1968, pp. 549-553.

7. Fumagalli, E., Verdelli, G. and Scotto, F.L., "PCPV for BWR: Experimental Investigations Up to Collapse of 1:10 Scale Model, Proceedings of SMIRT4, Vol. H, Paper H4/5, San Francisco, 1977.

8. Harvey, J.F., "Pressure Vessel Design - Nuclear and Chemical Applications", D. Van Nostrand Co. Inc., Princeton, N.J., 1963, pp. 202-246.

9. Hawkins, N.M., Wyss, A.N. and Mattock, A.H., "Fracture Analysis of Cracking in Concrete Beams", Journal of the Structural Division, ASCE, Vol. 103, No. ST5, May 1977, pp. 1015-1030.

10. Keenan, J.H., "Thermodynamics", The M.I.T. Press, Cambridge, Massachusetts, 1970.

11. Lange, N.A., "Handbook of Chemistry", Revised Tenth Edition, McGraw-Hill Book Co., New York, 1967, p. 1682.

12. McClintock, F.A. and Argon, A.S., "Mechanical Behavior of Materials", Addison-Wesley Publishing Company, Inc., Reading, Massachusetts, 1966.

13. Mershon, J.L., "Reinforcement of Openings Under Internal Pressure", Pressure Vessels and Piping Analysis - A Decade of Progress - Vol. 1, ASME, New York, N.Y., 1972, pp. 40-49.

14. Melville, J. and Foster, G.G., "A Pictorial Review of Failures in Conventional Boiler Plant", Pressure Vessels and Piping, An International Journal, Vol. 3, 1975, Applied Science Publishers, London.

15. Murray, D.W. and Epstein, M., "An Elastic Analysis of a Gentilly Type Containment Structure - Volume 1", Structural Engineering University of Alberta, Edmonton, Alberta, April 1976.

16. Orangun, C.O., Jirsa, J.O. and Breen, J.E., "A Re-evaluation of Test Data on Development Length and Splices", Journal American Concrete Institute, Proc. Vol. 74, No. 3, March 1977, pp. 114-122.

17. Poynor, J.F., "The Design of Conventional Pressure Vessels", in Pressure Vessel Engineering Technology, R.W. Nichols, Editor, Applied Science Publishers Ltd., London, 1971, pp. 1-56.

18. Perry, R.H. and Chilton, C.H., "Chemical Engineers' Handbook", Fifth Edition, McGraw-Hill Book Co., New York, N.Y., 1973.

19. Peterson, R.E., "Stress Concentration Factors", John Wiley and Sons, New York, 1974.

20. Rollins, J.P., Editor, "Compressed Air and Gas Handbook", Fourth Edition, Compressed Air and Gas Institute, 122 East 42nd Street, New York, N.Y., 10017, 1973.

21. Savin, G.N., "Stress Concentration Around Holes", Translated from the Russian by E. Gros, Pergamon Press, London, 1961.

22. Tate, L.A. and Smith, J.R., "Design of Vessel Penetrations - Theory and Practice", Conference on Prestressed Concrete Pressure Vessels, The Institute of Civil Engineers, London, 1968.

TABLES

TABLE 1 - ENERGY IN PNEUMATIC LOADING

PRESSURE (psig)	PRESSURE (psfa)	ENERGY[a] (FT-LB/FT.^{3})	TEST STRUCTURE[b]		GENTILLY-2[c]	
			TOTAL ENERGY (FT-LB)	$h_{equ.}$ of DOME (FT)	TOTAL ENERGY (FT-LB)	$h_{equ.}$ of DOME (FT)
0	0	0	0	0	0	0
20	4997	2718	2.3×10^6	568	6.66×10^9	372
40	7877	6163	5.2×10^6	1288	15.1×10^9	843
60	10757	9991	8.5×10^6	2083	24.5×10^9	1368
80	13637	14070	12.0×10^6	2941	34.5×10^9	1927
100	16517	18333	15.6×10^6	3833	44.9×10^9	2508

NOTES:
a. Computed from Eq. 4.2 with k = 1.4
b. Volume of air = 851 ft.^{3}; Weight of dome = 4070 lb-f.
c. Volume of air = 2.45×10^6 ft.^{3}; Weight of dome = 17.9×10^6 lb-f.

TABLE 2 - ENERGY IN HYDRAULIC LOADING
OF U. OF A. TEST STRUCTURE

Pressure psig	Dissolved Air $\frac{\text{ft.}^3 \text{ @ 20°C \& 1 atmo.}}{\text{ft.}^3 \text{ water}}$	Vol. Out of Soln. $\frac{\text{ft.}^3 \text{ @ 20°C \& 1 atmo.}}{851 \text{ ft.}^3 \text{ water } (v_2)}$	Total Vol. @ Pressurization ft.^{3} (v_1)	Total Energy Release ft-lb x 10^3	$h_{equiv.}$ of Dome ft.
0	0.020	0	0	0	0
20	0.047	23.0	9.7	41.7	10
40	0.074	46.0	12.4	128	31
60	0.102	69.8	13.7	240	59
80	0.129	92.8	14.4	365	90
100	0.156	115.7	14.8	496	122

TABLE 3 - ENERGY OF COMPRESSION IN PURE WATER

RELATIVE VOLUMES [11]: 1 atmo. & 20°C = 1.0016

500 atmo. & 20°C = 0.9804

@ 100 psig (7.80 atmo.) & 20°C = $1.0016 - \left\{\frac{7.8 - 1}{500 - 1}\right\} \times 0.0212 = 1.0013$

$\therefore$ $\Delta V/V$ @ 100 psi & 20°C = 0.0003/1.0016 = 0.0003

ENERGY/UNIT VOL. @ 100 psig = $100 \times 144 \times \frac{0.0003}{2} = 2.16$ psf

TOTAL ENERGY IN TEST STRUCTURE = 1840 ft-lb.

h_{equ} = 1840/4070 = 0.45 ft.

TABLE 4 - Summary of Equations
for Simple Section Analysis

LIMIT STATE	MEMBRANE FORCE	STRAIN[a]
1. ZERO CONCRETE STRESS	$P_o = A_s \left\{ f_{si} - n f_{ci} \right\} + A_p \left\{ f_{pi} - n f_{ci} \right\}$	$\varepsilon_o = -f_{si}/E_s$
2. CRACKING	$P_c = A_s \left\{ f_{si} + n (f_t - f_{ci}) \right\} + A_p \left\{ f_{pi} + n (f_t - f_{ci}) \right\} + A_c f_t$	$\varepsilon_c = (nf_t - f_{si})/E_s$
3. REINFORCEMENT YIELD	$P_y = A_s f_{sy} + A_p \left\{ f_{pi} + f_{sy} - f_{si} \right\}$	$\varepsilon_y = (f_{sy} - f_{si})/E_s$
4. ULTIMATE LOAD	$P_u = A_s f_{sy} + A_p f_{pu}$	$\varepsilon_u = (f_{pu} - f_{pi})/E_s$

Note a: $E_s = E_p$: $n = E_s/E_c$*

TABLE 5 - Percentage of Prestressing (ρ_p) Required to Arrest Brittle Fracture Prior to Attaining Ultimate Strength ($\beta = 0.6$)

f_{cu} f_t n	4500. 402. 7.7	5000. 424. 7.3	5500. 445. 7.0	6000. 465. 6.7	6500. 484. 6.4
ρ_s	ρ_p				
0.000	0.00953	0.01004	0.01053	0.01100	0.01145
0.001	0.00852	0.00903	0.00952	0.00999	0.01044
0.002	0.00753	0.00804	0.00853	0.00899	0.00944
0.003	0.00656	0.00707	0.00755	0.00802	0.00846
0.004	0.00560	0.00611	0.00659	0.00706	0.00750
0.005	0.00467	0.00517	0.00565	0.00611	0.00655
0.006	0.00375	0.00425	0.00473	0.00518	0.00562
0.007	0.00285	0.00334	0.00381	0.00427	0.00470
0.008	0.00196	0.00245	0.00292	0.00336	0.00379
0.009	0.00108	0.00157	0.00203	0.00247	0.00290
0.010	0.00022	0.00070	0.00115	0.00159	0.00202
0.011	0.0	0.0	0.00029	0.00073	0.00114
0.012	0.0	0.0	0.0	0.0	0.00028
0.013	0.0	0.0	0.0	0.0	0.0
0.014	0.0	0.0	0.0	0.0	0.0
0.015	0.0	0.0	0.0	0.0	0.0
0.016	0.0	0.0	0.0	0.0	0.0
0.017	0.0	0.0	0.0	0.0	0.0
0.018	0.0	0.0	0.0	0.0	0.0
0.019	0.0	0.0	0.0	0.0	0.0
0.020	0.0	0.0	0.0	0.0	0.0

Note: $f_y = 60000$ psi
$f_{pu} = 255000$ psi
$f_{pi} = 153000$ psi

TABLE 6 - Percentage of Prestressing (ρ_p) Required to Arrest Brittle Fracture Prior to Attaining Ultimate Strength ($\beta = 0.7$)

f_{cu} f_t n	4500. 402. 7.7	5000. 424. 7.3	5500. 445. 7.0	6000. 465. 6.7	6500. 484. 6.4
ρ_s	ρ_p				
0.000	0.01743	0.01877	0.01927	0.02012	0.02095
0.001	0.01537	0.01631	0.01720	0.01805	0.01887
0.002	0.01352	0.01445	0.01532	0.01617	0.01698
0.003	0.01182	0.01273	0.01360	0.01442	0.01522
0.004	0.01025	0.01113	0.01198	0.01279	0.01358
0.005	0.00877	0.00963	0.01046	0.01126	0.01202
0.006	0.00736	0.00821	0.00902	0.00980	0.01055
0.007	0.00603	0.00685	0.00764	0.00840	0.00914
0.008	0.00475	0.00555	0.00633	0.00707	0.00779
0.009	0.00352	0.00430	0.00506	0.00578	0.00649
0.010	0.00233	0.00310	0.00383	0.00454	0.00523
0.011	0.00119	0.00193	0.00265	0.00334	0.00401
0.012	0.00007	0.00080	0.00149	0.00217	0.00283
0.013	0.0	0.0	0.00037	0.00103	0.00168
0.014	0.0	0.0	0.0	0.0	0.00055
0.015	0.0	0.0	0.0	0.0	0.0
0.016	0.0	0.0	0.0	0.0	0.0
0.017	0.0	0.0	0.0	0.0	0.0
0.018	0.0	0.0	0.0	0.0	0.0
0.019	0.0	0.0	0.0	0.0	0.0
0.020	0.0	0.0	0.0	0.0	0.0

Note: $f_y = 60000$ psi
$f_{pu} = 255000$ psi
$f_{pi} = 178500$ psi

TABLE 7 - Minimum Percentages of Steel (ρ_g) to Prevent Yield Upon Brittle Fracture of the Concrete

f'_c	f_t	n	ρ_g
4500	402	7.7	0.015
5000	424	7.3	0.016
5500	445	7.0	0.017
6000	465	6.7	0.017
6500	484	6.4	0.018

Note: $f_{sy} = 60000$

$f_t = 6\sqrt{f'_c}$

$E_c = 57000\sqrt{f'_c}$

FIGURES

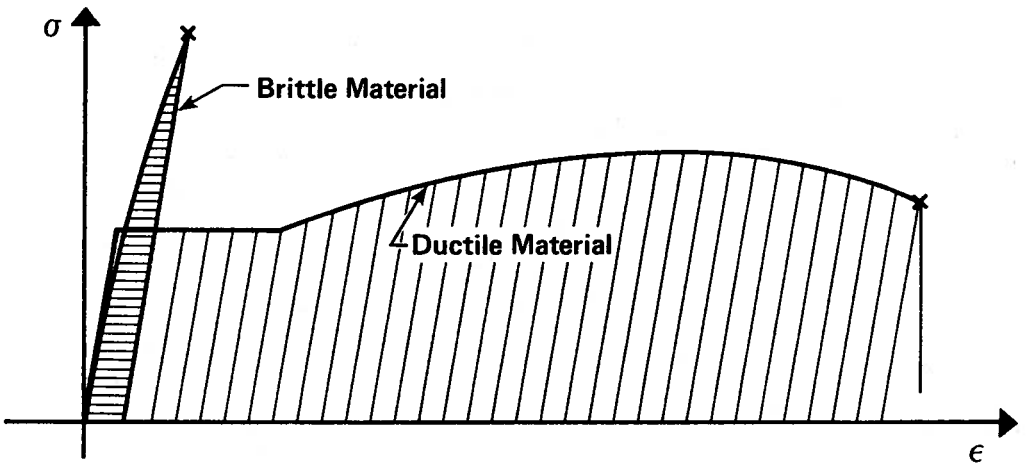

Fig. 1 Ductile and Brittle Stress-Strain Curves

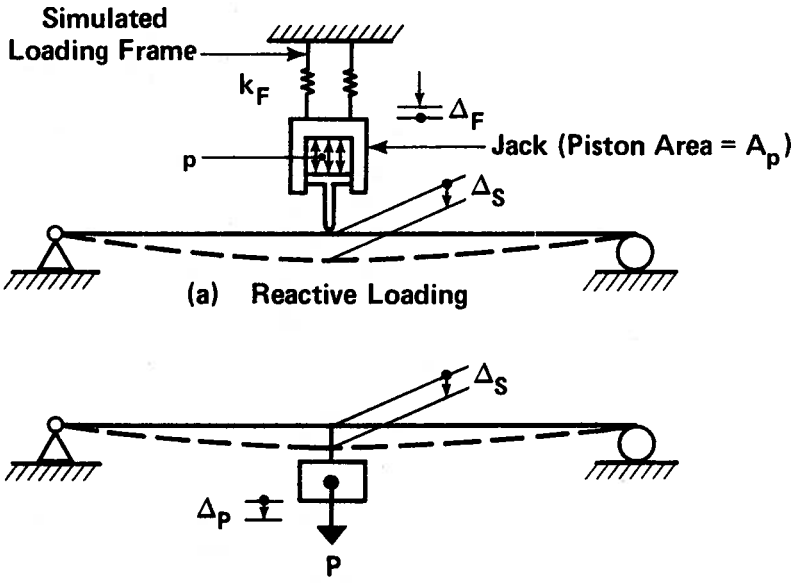

Fig. 2 Loading Systems

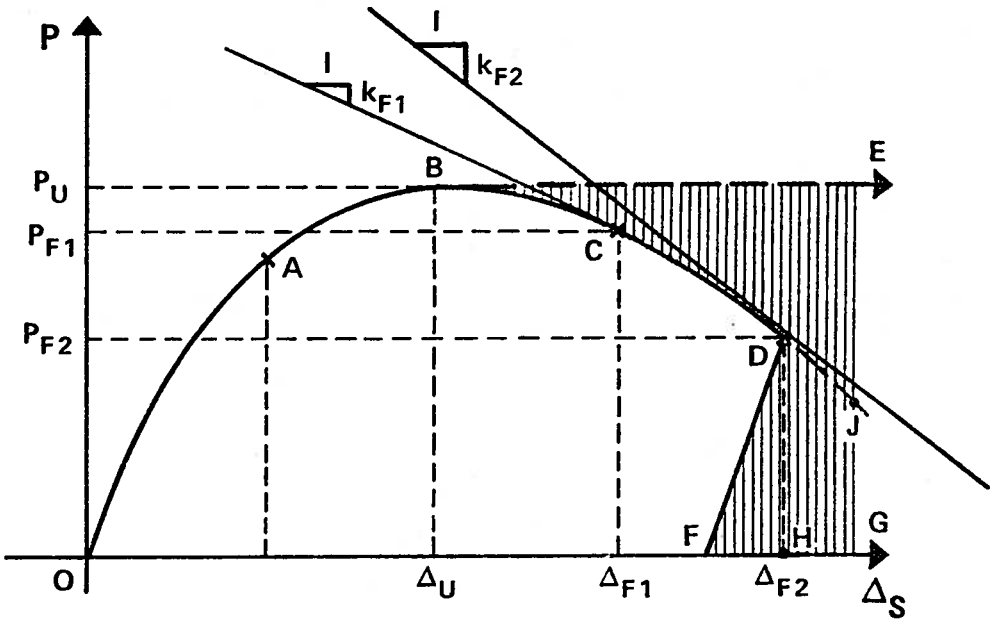

Fig. 3 Load-Deflection Curves

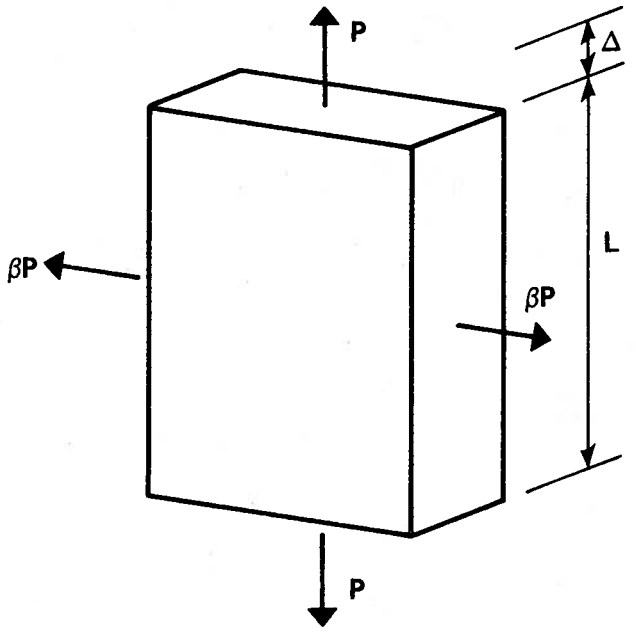

Fig. 4 Segment Loads and Deflection

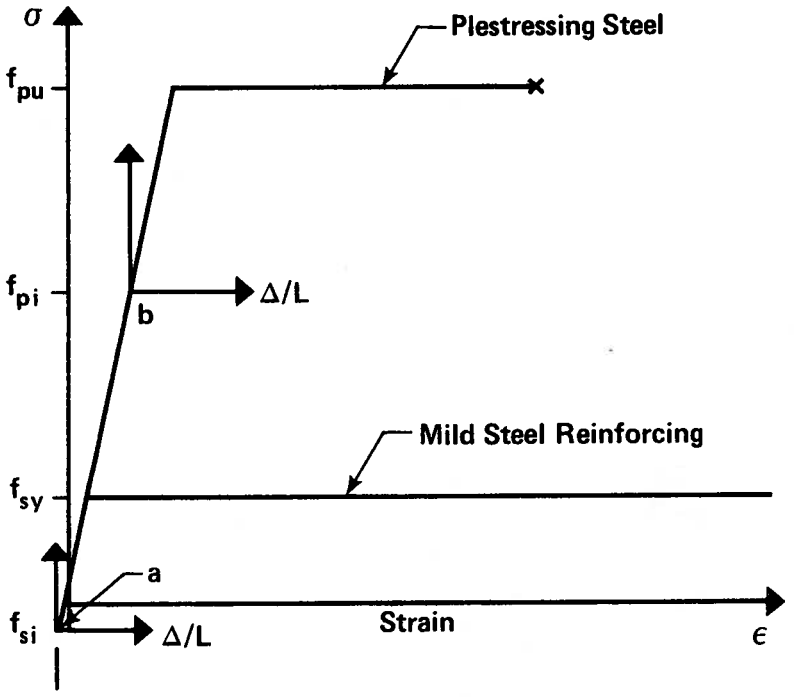

Fig. 5 Steel Stress-Strain Curves

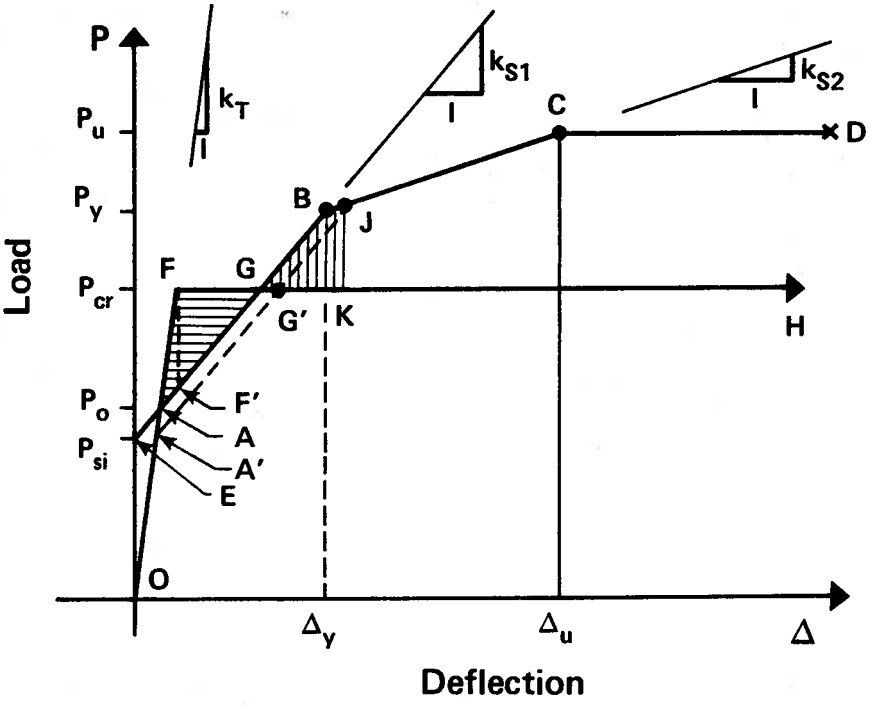

Fig. 6a Constrained Brittle Fracture

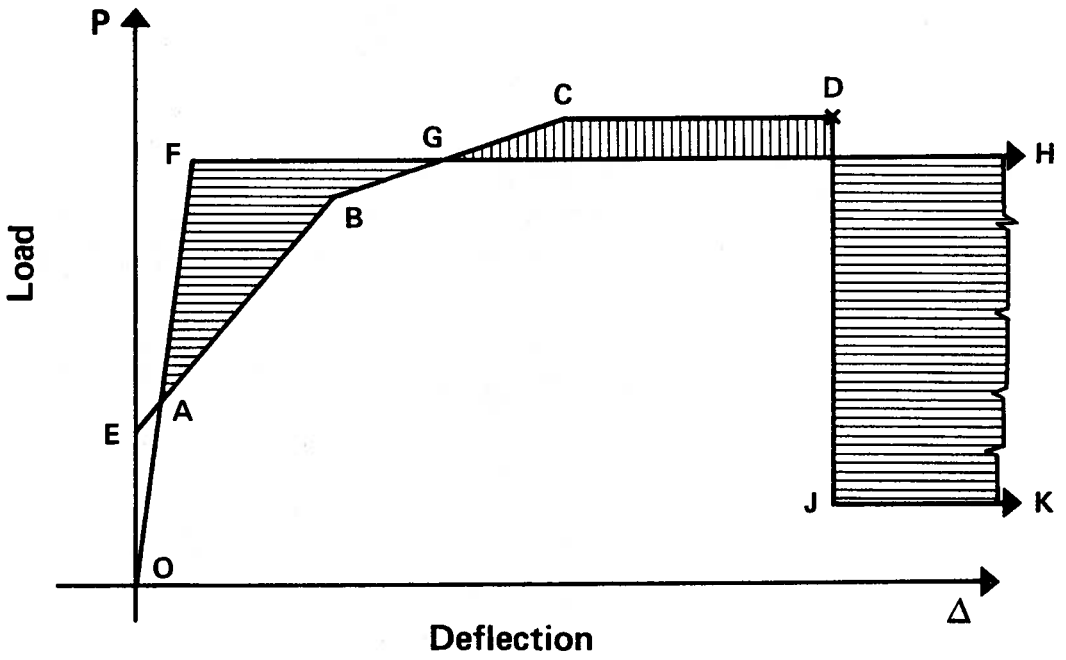

Fig. 6b Unstable Brittle Fracture

Fig. 6 Energy Relations for Brittle Tensile Failures

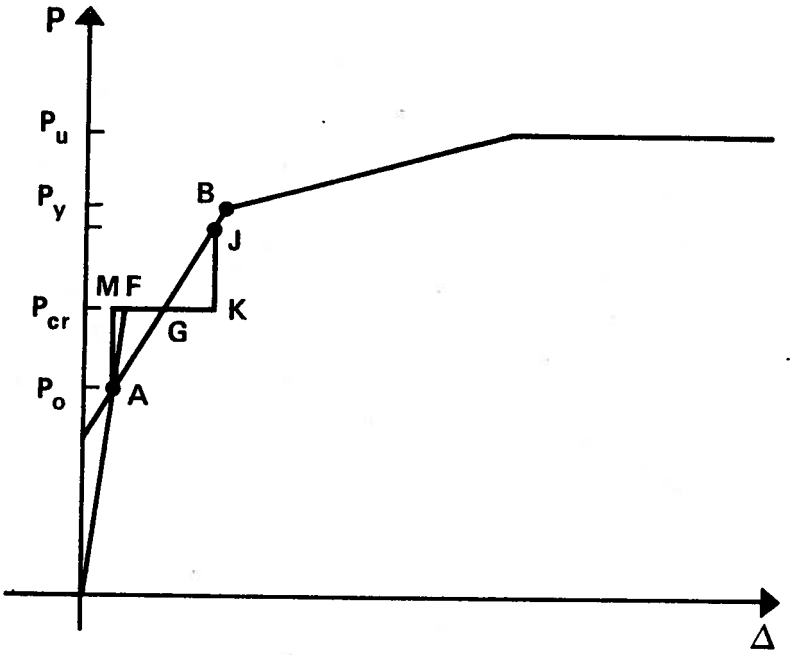

Fig. 7a Yield Limitation

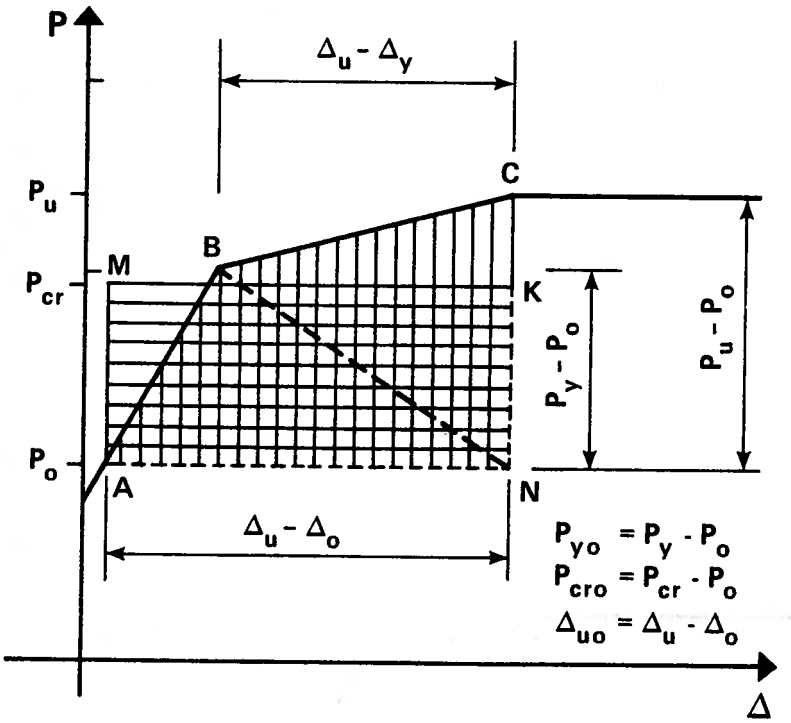

Fig. 7b Ultimate Limitation

Fig. 7 Energy Balances for Brittle Tensile Failures

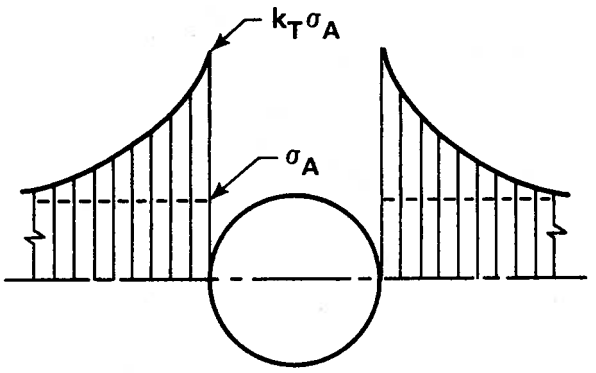

(a) Stress Concentration Around Circular Hole

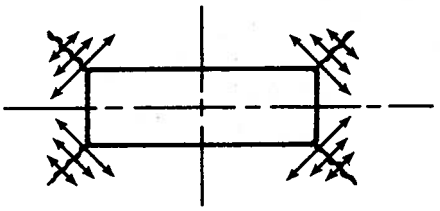

(b) Schematic Result of Stress Concentrations Around Rectangular Hole

Fig. 8 Stress Concentration Effects Around Penetrations

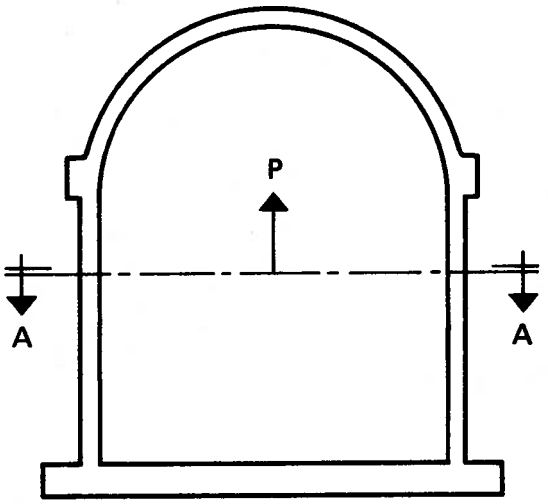

(a) Containment Structure

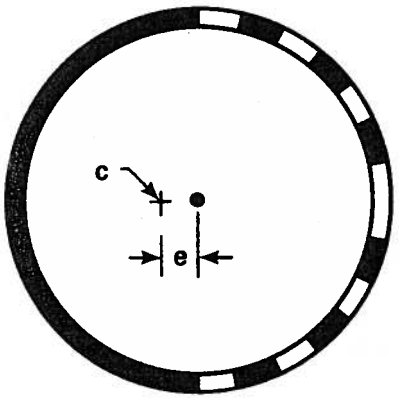

(b) Sect. A-A

Fig. 9 Eccentricity Due to Penetrations

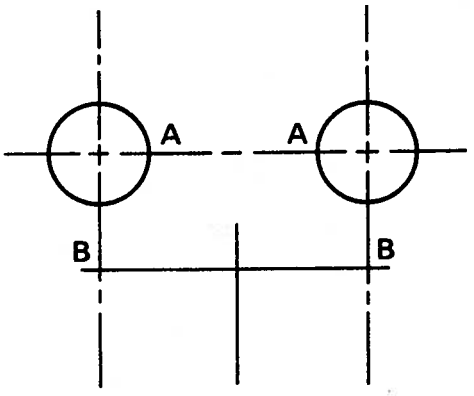

Fig. 10 Adjacent Penetrations

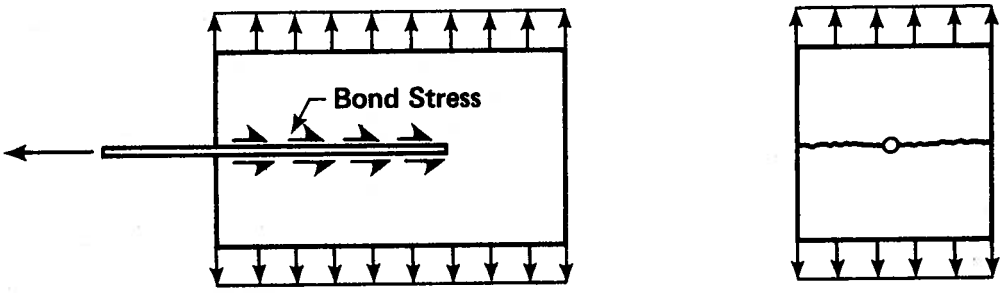

(a) Anchorage

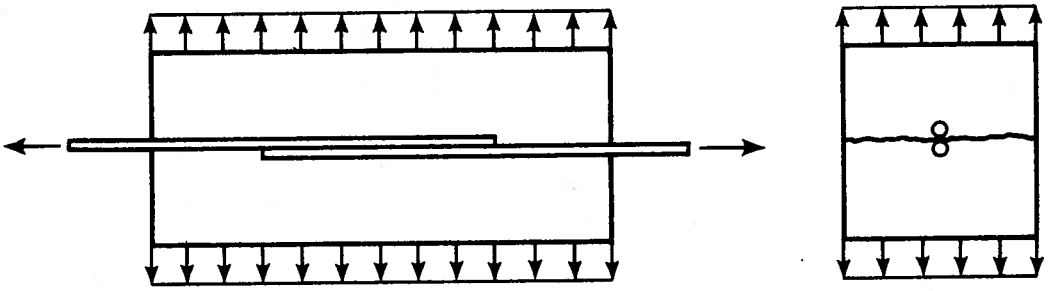

(b) Lap Splice

Fig. 11 Anchorage and Splicing of Reinforcement